Hydraulic Anisotropy Behavior of Compacted Soil

Harianto Rahardjo, Alfrendo Satyanaga, Leong Eng Choon
School of Civil and Environmental Engineering], Nanyang Technological University, Singapore, chrahardjo@ntu.edu.sg

Priono
Interdisciplinary Graduate School and Residues & Resource Reclamation Centre, Nanyang Environment & Water Research Institute, Nanyang Technological University, Singapore

ABSTRACT: Analysis of water flow in unsaturated soils is very important in many geotechnical applications. Many seepage analyses commonly assume soils are isotropic in order to simplify the numerical analyses. However, the hydraulic anisotropy behavior of a soil in the field can be a significant factor in affecting water flow within soil layer during rainfall. Previous research has not studied comprehensively the hydraulic anisotropy behavior of unsaturated soil. In this study, laboratory experiments were carried out on horizontal-layering (HL) and vertical-layering (VL) compacted soil specimens. The scope of the study included determination of soil-water characteristic curve using Tempe cell and determination of saturated permeability using conventional triaxial cell. The results indicated that hydraulic anisotropy can be associated with the ratio of the equalization time during SWCC tests between HL and VL specimens. The soil specimen compacted at wet of optimum has a higher hydraulic anisotropy as compared to that compacted at dry of optimum. In addition, the soil with a higher percentage of fine particles has a lower hydraulic anisotropy as compared to that with a lower percentage of fine particles.

KEYWORDS: hydraulic anisotropy, laboratory experiments, soil-water characteristic curve, saturated permeability

1 INTRODUCTION

Water flow through unsaturated soil zone has been associated with a variety of geotechnical and geo-environmental problems. Previous research works indicated that hydraulic anisotropy has a significant effect on the water flow within soil layer, especially within unsaturated soil zone (Priono et al. 2016). Soil-water characteristics curve (SWCC) and permeability function are the primary hydraulic properties in unsaturated soil. SWCC describes the capacity of water being stored within the macro- and micro-pores of a soil at different matric suctions (Fredlund et al. 2012). Coefficient of permeability relates flow rate to driving potential, mainly due to pressure head gradient, of a particular phase of the soil medium (Fredlund et al. 2012). Direct measurement of permeability function is tedious and very time-consuming (Leong and Rahardjo 1997). Hence, permeability function is commonly determined indirectly using statistical method (Childs and Collis-George 1950).

Hydraulic anisotropy of soil is defined as a ratio of water coefficients of permeability on major to minor axes of soil (Mualem 1986; Chapuis et al. 1989; Bear and Cheng 2010). The water flow that is parallel to layering of soil is represented by major axis whereas the water flow that is perpendicular direction to layering is represented by minor axis. Hydraulic anisotropy of a soil may either equal to one (isotropic), larger or less than one (anisotropic).

Past studies on hydraulic anisotropy have focused on saturated soil (Basak 1972 and Chapuis et al. 1989). Limited research works were carried out on hydraulic anisotropy for soil under unsaturated condition. Priono et al. (2016) investigated the hydraulic anisotropy characteristics of a coarse-grained soil under unsaturated condition via numerical analyses and laboratory tests. They compacted and trimmed the soil to produce horizontal-layering (HL) and vertical-layering (VL) soil specimens to understand the effect of hydraulic anisotropy (directional-dependence) on SWCC (Priono et al. 2016).

The objective of this study is to investigate the hydraulic anisotropy behavior of a fine-grained soil under unsaturated condition. The scope of works include measurement of SWCC in laboratory using Tempe cell and measurement of saturated permeability using triaxial cell with two back pressure systems.

2 MATHEMATICAL EQUATION

Several mathematical equations have been proposed to best fit SWCC (Fredlund et al., 2012). Since soils with unimodal and bimodal SWCC were used in this study, Satyanaga et al. (2013) equations were used for best fitting unimodal (see Eq. 1) and bimodal SWCC (see Eq. 2).

$$\theta_w = \left(1 - \frac{\ln\left(1+\frac{\psi}{\psi_r}\right)}{\ln\left(1+\frac{10^6}{\psi_r}\right)}\right)\left[\theta_r + \left\{(\theta_s - \theta_r)\left(1-(\beta)erfc\left(\frac{\ln\left(\frac{\psi_a-\psi}{\psi_a-\psi_m}\right)}{s}\right)\right)\right\}\right] \quad (1)$$

$$\theta_w = \left(1 - \frac{\ln\left(1+\frac{\psi}{\psi_r}\right)}{\ln\left(1+\frac{10^6}{\psi_r}\right)}\right)\left[\begin{array}{l}\theta_r + (\theta_{s1} - \theta_{s2})\left(1-(\beta_1)erfc\dfrac{\ln\left(\frac{\psi_{a1}-\psi}{\psi_{a1}-\psi_{m1}}\right)}{s_1}\right) \\ + (\theta_{s2} - \theta_r)\left(1-(\beta_2)erfc\dfrac{\ln\left(\frac{\psi_{a2}-\psi}{\psi_{a2}-\psi_{m2}}\right)}{s_2}\right)\end{array}\right] \quad (2)$$

where:
β = 0 when $\psi \le \psi_a$; β = 1 when $\psi > \psi_a$
θ_w = calculated volumetric water content
θ_s = saturated volumetric water content
ψ = matric suction under consideration (kPa)
ψ_a = parameter represents the air-entry value of soil (kPa)
ψ_m = parameter represents the matric suction at the inflection point of SWCC (kPa)
s = parameter represents the geometric standard deviation of SWCC
θ_r = parameter represents the residual volumetric water content
ψ_r = parameter represents the matric suction corresponding to residual volumetric water content (kPa)
erfc = the complimentary error function

β_1 = 0 when $\psi \leq \psi_{a1}$; $\beta 1$ = 1 when $\psi > \psi_{a1}$
β_2 = 0 when $\psi \leq \psi_{a2}$; $\beta 2$ = 1 when $\psi > \psi_{a2}$
Subscripts 1 and 2 represent subcurve 1 (associated with macro pore) and subcurve 2 (associated with micro pore), respectively.

The equalization time (i.e. time where the gradient of water volume change reached zero value for the first time at a particular suction) during SWCC test was obtained by Taylor Series' central difference estimation (Equation 3). The ratio of equilibrium time observed in HL and VL specimens reflects the hydraulic anisotropy of the unsaturated soil (Priono et al., 2016).

$$f'(x_i) = \frac{f'(x_{i+1}) - f'(x_{i-1})}{2h} + O(h^2) \quad (3)$$

where:
$f'(x_i)$ = gradient of SWCC at each applied suction;
h = step size (50 intervals);
$O(h^2)$ = truncation error.

3 LABORATORY TESTS

Laboratory tests were carried out using a mixture of L2-grade kaolin and 20-30 grade Ottawa sand of 70% and 30% by dry mass, respectively. The compacted soils were used in this study to avoid heterogeneity of the soil specimens for a high accuracy of analyses (Goh et al 2010, Indrawan et al. 2006). Standard Proctor compaction tests (ASTM D692-12e1) were used to obtain the compaction curve of the soil mixture. Static compaction was used to produce all soil specimens with 50 mm diameter cylindrical shape which were compacted in 10 mm layers at 1 mm/min static loading rate according to the procedure described in Ong (1999). Static compaction was used to ensure uniform compaction, homogeneity and reproducibility of specimens for different type of tests.

Two sets of soil specimens were used in this study to investigate the hydraulic anisotropy behavior at different water contents with respect to the same dry density of soil specimen. The first set of specimens consists of HL and VL specimens compacted at the dry of optimum associated with 95% of maximum dry density ($\rho d,max$) (Specimen A) whereas the second set of specimens consists of HL and VL specimens compacted at the wet of optimum associated with 95% of $\rho d,max$ (Specimen B). The preparation of HL and VL specimens followed the procedures explained in Priono et al (2016) and Chapuis and Gill (1989).

Index properties of the soil mixture including specific gravity, Atterberg limits, grain size distribution and soil classification according to the Unified Soil Classification System (USCS) were conducted according to ASTM D854-14 (2014), ASM D4318-10e1 (2010), ASTM D422-63e2 (2007) and ASTM D2487-11 (2011), respectively.

In this study, the SWCC was determined using Tempe cell tests following ASTM D6838-02 (2008). The main part of the Tempe cell is the high air-entry porous ceramic plate. Prior to the test, the ceramic plate was saturated in a desiccator with de-aired distilled water under vacuum. The specimen was weighed every day until the weight of the specimen remained unchanged before increasing the matric suction to the next value.

In this research, saturated permeability tests were carried out in a triaxial cell with two back pressure systems (Head 1986). Two back pressure systems were used to cause de-aired distilled water to flow upward through the specimen under an intended pressure head difference i.e. 5 and 10 kPa. Two different pressure head gradients were. The experiment was stopped when water inflow to the soil specimen was equal to water outflow from the soil specimen over a period of time.

4 RESULTS AND DISCUSSIONS

The grain-size distribution of soil specimen used in this study is presented in Figure 1. The grain-size distribution curve illustrates that 20-30 Ottawa sand consists predominantly of medium-sized sand whereas L2-grade kaolin consists mainly of silt-sized particles.

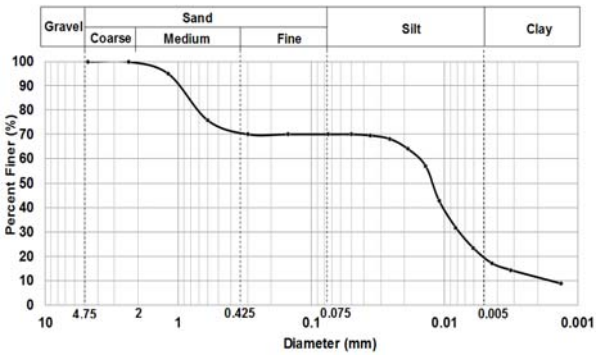

Figure 1. Grain-size distribution curve of soil specimen used in this study

Initial conditions of soil specimens used in the laboratory tests were obtained from the compaction curve of sand-kaolin mixtures (30S70K) as presented in Figure 2. The maximum dry density of 1.61 Mg/m3 is observed at the optimum water content of 19.5%. Index properties for soil specimens A and B prepared at 95% of maximum dry density associated with dry and wet of optimum, respectively, are listed in Table 1.

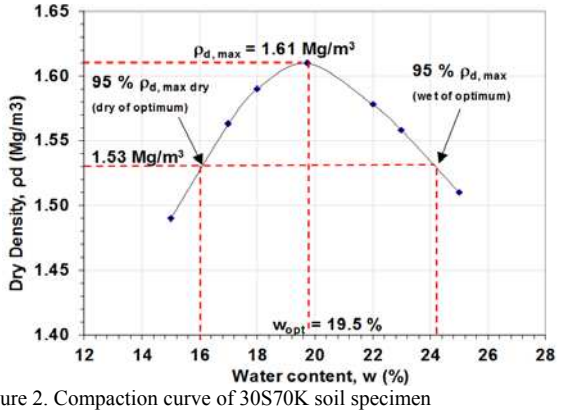

Figure 2. Compaction curve of 30S70K soil specimen

Table 1. Index properties of 30S70K soil specimen

Index properties	*Specimen A*	*Specimen B*
Dry density, ρ_d (Mg/m^3)	1.53	1.53
Water content, w (%)	16	24.2
Sand (%)	30	30
Silt (%)	63.4	63.4
Clay (%)	6.6	6.6
Liquid Limit, LL (%)	53	53
Plastic Limit, PL (%)	31	31
Plasticity Index, PI (%)	22	22
USCS	MH	MH

Saturated permeability of HL and VL of Specimens A and B are presented in Table 2 which shows that VL specimen had a higher saturated permeability as compared to HL specimen since water flowed much faster in VL specimen as compared to HL specimen to reach the datum which was at the bottom of the specimen, at a given head gradient. Table 2 also shows that Specimen B (compacted at wet of optimum) had a higher hydraulic anisotropy as compared to Specimen A (compacted at dry of optimum). This is attributed to a dispersed soil structure of specimen B, as explained in Fredlund and Rahardjo (1993), which can enhance hydraulic anisotropy.

Table 2. Saturated permeability of 30S70K soil specimen

Specimen	$k_{s,\,HL}$ *(m/s)*	$k_{s,\,VL}$ *(m/s)*	*Hydraulic anisotropy*
A	9.3e-9	2.0e-8	2.16
B	5.2e-10	2.2e-9	4.26

Figures 3 and 4 show SWCCs of Specimens A and B, respectively. It is observed that specimen A with an initial condition associated with the dry of optimum had a bimodal characteristic of SWCC whereas specimen B with an initial condition associated with the wet of optimum had a unimodal characteristic of SWCC. This observation agreed with previous works (Rahardjo et al., 2012; Satyanaga et al., 2013) which concluded that the shape of the SWCC of compacted soil may or may not follow the shape of GSD curve and depends on the initial conditions (water content and dry density).

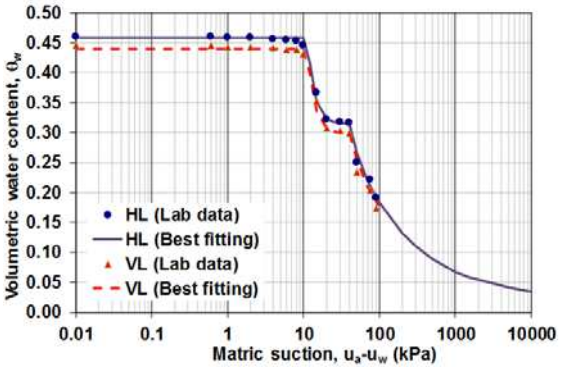

Figure 3. SWCCs of specimen A

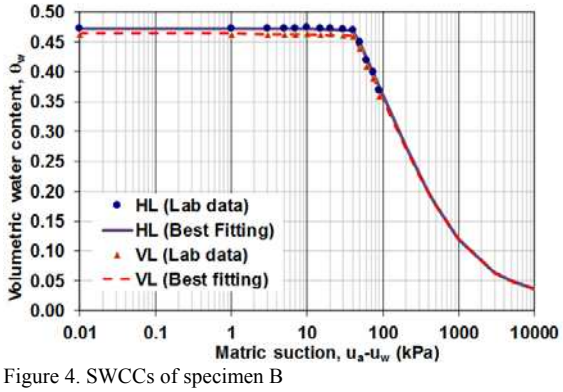

Figure 4. SWCCs of specimen B

Figures 3 and 4 show that HL and VL specimens have very similar SWCC data. Tables 3 and 4 indicate that HL and VL specimens can be best fitted using the same SWCC parameters of Equations (1) and (2) for unimodal and bimodal SWCCs, respectively, relatively well. This is expected since SWCC is a constitutive surface that relates equilibrium water contents with their corresponding matric suctions and this relationship is unique for a given soil regardless of different layering orientations and hydraulic anisotropies.

Table 3. Fitting SWCC parameters of specimen A

Parameters	*HL*	*VL*
θ_{s1}	0.458	0.440
ψ_{a1} (kPa)	10	10
ψ_{m1} (kPa)	13	13
s_1	0.75	0.75
θ_{s2}	0.315	0.300
ψ_{a2} (kPa)	40	40
ψ_{m2} (kPa)	100	100
s_2	2	2
ψ_r (kPa)	1000	1000
θ_r	0.050	0.050
R^2	0.995	0.997

Table 4. Fitting SWCC parameters of specimen B

Parameters	*HL*	*VL*
θ_s	0.473	0.464
ψ_a (kPa)	40	40
ψ_m (kPa)	250	250
S	1.85	1.85
θ_r	0.05	0.05
ψ_r (kPa)	700	700
R^2	0.998	0.996

The difference between HL and VL specimens is observed on the time required for achieving equilibrium (steady state) condition, usually termed as equalization time and occurs after air-entry value (AEV) of the specimen. Equalization time at the application of matric suction less than or around the AEV is relatively indifferent between HL and VL specimens since there is no significant change of water volume measured. Tables 5 and 6 show equalization time after the AEV for HL and VL of Specimens A and B, respectively. The general trend is equalization time during SWCC test increases with the increase in matric suction since pore-water connectivity inside a soil decreases.

Table 5. Equalization time of specimen A

Matric suction	*HL*	*VL*	*Ratio*
20	42.3	19.8	2.1
40	44.5	21.3	2.1
50	46.3	19.8	2.3
75	54.5	23.7	2.3
90	74.4	37.4	2.0

The equalization time ratio of Specimens A and B from SWCC tests (Tables 5 and 6) confirms the hydraulic anisotropy as obtained from saturated permeability tests. This result is in agreement with previous works by Priono et al. (2016). Study

by Priono et al. (2016) showed that the hydraulic anisotropy of specimen 50S50K compacted at 95% ρd,max at dry of optimum and wet of optimum were approximately 3.2 and 5.8, respectively. The results in this study show that the hydraulic anisotropy of specimen 30S70K compacted at 95% ρd,max at dry of optimum and wet of optimum were approximately 2.2 and 4.3, respectively. The comparison between the hydraulic anisotropy values of soil specimens 30S70K and 50S50K indicates that soil with a higher percentage of fine particles will give a lower hydraulic anisotropy. This may occur since soil specimen 30S70K has a lower initial dry density (1.53 Mg/m3) as compared to soil specimen 50S50K (1.75 Mg/m3). As a result, soil specimen 30S70K has a less compacted soil structure as compared to soil specimen 50S50K. Hence, the fine-grained soil has less variation of pore-water connectivity in different directions. Therefore, the fine-grained soil is less anisotropic as compared to the coarse-grained soil.

Table 6. Equalization time of specimen B

Matric suction	*HL*	*VL*	*Ratio*
50	69.3	17.0	4.1
75	94.0	21.7	4.3
90	163.0	41.0	4.0

5 CONCLUSIONS

The conclusions of this study are as follows:

1. SWCC is a scalar property which is not affected by the hydraulic anisotropy, given the same dry density.

2. Hydraulic anisotropy of soil is reflected by - the ratio of the equalization time between HL and VL specimens.

3. The soil specimen compacted at wet of optimum has a higher hydraulic anisotropy as compared to that compacted at dry of optimum. On the other word, soil with a higher water content has a higher hydraulic anisotropy as compared to the soil with a lower water content at the same dry density.

4. Soil with a higher percentage of fines has a lower hydraulic anisotropy as compared to soil with a lower percentage of fines, given the same dry density.

6 ACKNOWLEDGEMENTS

The authors gratefully acknowledge the assistance of Kevin Janiardy and Nickanor Tikno, School of Civil and Environmental Engineering, NTU, Singapore during the experiments and data collections.

7 REFERENCES

ASTM D2487-11. 2011. Standard practice for classification of soils for engineering purposes (Unified Soil Classification System). Annual Book of ASTM Standards, ASTM International, West Conshohocken, PA.

ASTM D422-63e2. 2007. Standard test method for particle-size analysis of soils. Annual Book of ASTM Standards, ASTM International, West Conshohocken, PA.

ASTM D4318-10e1. 2010. Standard test methods for liquid limit, plastic limit, and plasticity index of soils. Annual Book of ASTM Standards, ASTM International, West Conshohocken, PA.

ASTM D698-12e1. 2012. Standard test methods for laboratory compaction characteristics of soil using standard effort. Annual Book of ASTM Standards, ASTM International, West Conshohocken, PA.

ASTM D854-14. 2014. Standard test methods for specific gravity of soil solids by water pycnometer. Annual Book of ASTM Standards, ASTM International, West Conshohocken, PA.

ASTM D6838-02. 2008. Standard test methods for the soil–water characteristic curve for desorption using hanging column, pressure extractor, chilled mirror hygrometer, or centrifuge.

Bear, J. and Cheng, A.H.D. 2010. Modeling Groundwater Flow and Contaminant Transport. New York: Springer.

Chapuis, R.P and Gill,D.E. 1989. Hydraulic anisotropy of homogeneous soils and rocks: influence of the densification process. Engineering Geology, 39:75-86

Chapuis, R.P., Gill, D.E., Baass, K. 1989. Laboratory permeability tests on sand: influence of the compaction method on anisotropy. Canadian Geotechnical Journal, 26:614-622.

Childs, E.C. and Collis-George, G.N. (1950). "the Permeability of porous materials." Proc. Royal Soc. Of London, Series A, London, UK, 201, 392-405.

Fredlund, D.G., H. Rahardjo and M.D. Fredlund (2012). "Unsaturated Soil Mechanics in Engineering Practice". John Wiley & Sons, Inc., New York, 926 pages (ISBN 978-1-118-13359-0).

Fredlund D.G., Rahardjo H. (1993), Soil Mechanics for Unsaturated Soils, John Wiley & Sons, New York, pp.517.

Goh SG, Rahardjo H, Leong EC. Shear strength equations for unsaturated soil under drying and wetting. J Geotech Geoenviron Eng 2010;136(4):594–606.

Head, K. H. (1986), Manual of Soil Laboratory Testing. Vol 3: Effective Stress Tests, London, pp. 743–1238.

Indrawan IGB, Rahardjo H, Leong EC. Effects of coarse-grained materials on properties of residuals soil. J Eng Geol 2006;82(3):154–64.

Mualem, Y. 1986. Hydraulic conductivity 493 of unsaturated soils: prediction and formulas. Methods of Soil Analysis, Part 1: Physical and Mineralogical Methods. 2nd Edition, Agronomy. American Society of Agronomy, Inc., and Soil Science Society of America, Madison, 799–823.

Ong, B. H. 1999. Shear strength and volume change of unsaturated residual soil. MEng Thesis, Nanyang Technological University, Singapore.

Priono et al. (2016), "Effects of Hydraulic Anisotropy on Soil-Water Characteristics Curve," Soils and Foundations, Vol. 56, No 2, pp. 228-239.

Rahardjo, H., Satyanaga, A., D'Amore, G.A.R., Leong, E.C. 2012. Soil-water characteristic curves of gap-graded soils. Engineering Geology, 125:102-107.

Satyanaga, A., Rahardjo, H., Leong, E.C. and Wang, J.Y. "Water Characteristic Curve of Soil with Bimodal Grain-Size Distribution," Computers and Geotechnics, Vol. 48, pp. 51-61, 2013.